DOI Link: https://doi.org/10.61586/1e5bi
Vol.43, Issue.8, Part.1, August 2025, PP.50-83

BIOSYNTHESIS OF SILVER NANOPARTICLES FROM *SARGASSUM MUTICUM* EXTRACT AND ITS COMPATIBILITY WITH *TRICHODERMA HARZIANUM* FOR CONTROLLING THE TOMATO LEAF MINER, *TUTA ABSOLUTA*

Alaa Baazeem[a], H. Darwish[b], R. A. Algotiml[c,d], A. Alghamdi[a], S. S. Alhelaify[b], A. S. Alswat[b], M. A. Alghamdi[b], M. Alorabi[b], W. M. Al-Otaibi[a], A. S. Alqurashi[a], M. M. Hassan[a], R. H. Alghamdi[e], H. Elshazly[f,g], M. A. Farid[h], N. M. Almasoudi[i], M. A. Osman[j,k], Z. M. Al Dhafar[j,k], N. H. Ashri[l], A. Noureldeen[a,*]

[a] Department of Biology, College of Sciences, Taif University, Taif 21944, Saudi Arabia
[b] Department of Biotechnology, College of Sciences, Taif University, Taif 21944, Saudi Arabia
[c] Department of Biology, Faculty of Applied Science, Umm Al-Qura University, Makkah, Saudi Arabia
[d] Research Laboratories Unit, Faculty of Applied Science, Umm Al-Qura University, Makkah, Saudi Arabia.
[e] Department of Chemistry, Collage of Science, Taif University, P.O.BOX 11099, Taif 21944, Saudi Arabia
[f] Biology Department, Faculty of Sciences & Arts-Scientific Departments, Qassim University, Qassim 52571, Saudi Arabia
[g] Zoology Department, Faculty of Science, Beni-Suef University, Beni-Suef 62521, Egypt
[h] Genetics Department, Faculty of Agriculture, Kafrelsheikh University, Kafr Elsheikh 33516, Egypt
[i] Department of Agriculture, Faculty of Environmental Sciences, King Abdulaziz University, Jeddah 21551, Saudi Arabia
[j] Department of Biology, College of Science, Imam Abdulrahman Bin Faisal University, P.O. Box 1982, Dammam 31441, Saudi Arabia
[k] Basic and Applied Scientific Research Center (BASRC), Imam Abdulrahman Bin Faisal University, P.O. Box 1982, Dammam 31441, Saudi Arabia
[l]Department of Biology, Faculty of Sciences, Umm Al Qura University, Makkah, Saudi Arabia
* Corresponding author: a.noureldeen@tu.edu.sa

Received Feb 2025 Accepted July 2025 Published August 2025

ABSTRACT

A worldwide destructive pest that has an impact on tomato output is the tomato leaf miner, *Tuta absoluta*. Biosynthesized nanoparticles and entomopathogenic fungi (EFs) are widely recognized for their ability to regulate the development and emergence of this insect pest. The goal of the current investigation was to synthesize, characterize, and evaluate the bio-fabricated silver nanoparticles from the brown alga, *Sargassum muticum* extract either singly or combined with the locally entomopathogenic fungus (EF), *Trichoderma harzianum* against *T. absoluta*. A color change was detected by visual examination of the surface plasmonic band of the biosynthesized AgNPs capped with *S. muticum* extract, which peaked at 407 nm using UV-Vis spectroscopy. Transmission electron microscopy (TEM) revealed that the AgNPs had a spherical, oval, and hexagonal shape with a nanoscale size of 11 nm. Analysis of fourier transform infrared (FTIR) spectroscopy revealed that multiple molecules were bonded to AgNPs via CH_2, C=O, and C=C groups. The zeta potential of prepared silver nanoparticle is -20.6 mV. Energy-dispersive X-ray spectroscopy (EDX) analysis indicate the presence of Ag, C, O_2, k, Cl, S, Si, Mg, and Na substances, and Ag was the main element, accounting for approximately 9.08% of mass, as evidenced by an intense signal at 2.983 KeV. The isolated fungus was molecularly identified as *T. harzianum* T1. The major constituent of the fungal filtrate was 6,8-dibromo-2-(3-pyridyl)-4-phenyl-quinazoline (70.31%). The results showed an overall good insecticidal activity (39.0-92.0% mortality) of the compounds tested when applying individually for three days, with a higher mortality on larvae over pupae. The *S. muticum*-AgNPs was compatible with conidial suspension or filtrate of *T. harzianum* T1 with larval mortality percentage of 96.0 or 85.2% 72 h-post treatments. The data collected suggest that these compounds, especially when nanoformulated combined with fungal conidia, could be effectively applied to *T. absoluta* integrated pest management strategies.

KEYWORDS:

Alga-synthesized silver nanoparticles, Entomopathogenic fungi, GC-MS analysis, *Tuta absoluta*, Bioactivity.

INTRODUCTION

The urgent requirement to improve agricultural sustainability has forced researchers, the agroindustry, farmers, and consumers to look for creative ways to reduce the need for agrochemicals while maintaining the highest possible crop yields (Minchev et al., 2024). Global agricultural food production is seriously threatened by invasive insect pests (Skendžić et al., 2021). The tomato leaf-miner (TLM), *Tuta absoluta* (Meyrick, 1917) (Lepidoptera: Gelechiidae) is a highly destructive insect pest that attacks tomato plants and other solanaceous crops (Zhang et al., 2020; Erasmus et al., 2021; Bakheit et al., 2022), causing yield losses of up to 100% estimated at USD 1.1 billion worldwide annually if uncontrolled under both greenhouse and open-field conditions (Pratt et al., 2017; Biondi et al., 2018; Vivekanandhan et al., 2024). The most popular method of controlling pests among farmers is the use of chemical insecticides (Tarusikirwa et al., 2020). However, because of documented resistance, possible negative impacts on the environment and human health, and indirect effects on natural enemies, this management strategy can be costly and occasionally ineffectual (Krache et al., 2022). Additionally, the effectiveness of synthetic pesticides is limited by the mine-feeding behavior of *T. absoluta* larvae (Gebremariam, 2015). In addition to being dangerous, chemical pesticides' limited effectiveness makes integrated pest management (IPM) and the application of pest control measures that guarantee favorable sociological, ecological, and economic outcomes necessary. Farmers can reduce *T. absoluta* populations by using entomopathogens and nano-based biopesticides (Abd El-Ghany et al., 2018).

Numerous specific features of metals, polymers, and metallic alloys—both natural and synthetic—make them perfect for a range of agricultural and biological applications (Judith Vijaya et al., 2017; Usman et al., 2020). Several studies have shown the synthesis of nanoparticles by seaweeds and their biological applications, as well as cytotoxicity (Ananthi et al., 2010; Arya and Chundawat, 2018; Jeyarani et al., 2020; Usman et al., 2020). Chemical and physical processes are used to synthesize metal nanoparticles, which allow them to have desired properties. Metal nanoparticles can be synthesized in a variety of ways, including conventional heating, anodization, deposition precipitation, oxidation, and hydrothermal processes (Badineni et al., 2021). As well, these methods of synthesis are usually labor-intensive, expensive, and dangerous. Compared to physical and chemical methods, green nanoparticle synthesis is eco-friendly, cost-effective, easy to scale, doesn't need harmful substances, high temperatures, or energy, and is more efficient. Nanoparticles produced via green synthesis have better influence, stability, controlled growth, and crystal development (Valsalam et al., 2019; Mani et al., 2021). The green synthesized nanoparticles have antibacterial, antifungal, cytotoxic, and photochemical applications (Sathiyaraj et al., 2021; Bensy et al., 2022; Viswanathan et al., 2024). Kannan et al. (2013) created silver nanoparticles by the extract of seaweed (*Chaetomorpha linum*), and recorded that it has the potential to be used in biomedicine and agriculture and is safe for the environment. The silver nanoparticle synthesized from marine algae *C. linum* was a potent anticancer drug that may cause colon cancer cells (HCT-116) to apoptosis (Acharya et al., 2021). Moreover, Somu et al. (2022) produced ZnO nanoparticles using the brown algae

C. linum as a reductant; the absorption peak maximum was detected at 356.8 nm. Additionally, the brown seaweed *Sargassum muticum* extract was found to be a successful capping agent for creating AgNPs, which can be employed in industry as an antimicrobial and dye adsorbent agent as well as to prevent dangerous mosquito vectors (Trivedi et al., 2021). Similarly, Moorthi et al. (2015) used *S. muticum* extract to create AgNPs and found that the phytochemicals in *S. muticum* were a key precursor for the production of highly efficient nanoparticles against *Ergolis merione* insect. Furthermore, *S. muticum*-mediated nanoparticles and their nanocomposites were proved to be photocatalytic and photoexcited anti-microbial agents (Harinee et al., 2022). On the other hand, the two red algae, *Laurencia papillosa* and *Galaxaura rugosa*-fabricated silver nanoparticles were successfully synthesized by a simple and safe reduction method (El Shehawy et al., 2023). In the same context, a marine sponge *Carteriospongia foliascens*, along with marine natural extracts of two red algae (*Bostrychia tenella* and *L. obtusa*), a green alga (*Halimeda tuna*), and a brown alga (*S. filipendula*), were used to create titanium dioxide (TiO_2) nanoparticles using a novel green chemistry technique, and its applications as eco-friendly antifouling agents were also recoded (Alarif et al., 2023). Metallic and non-metallic nanoparticles have shown great promise for lowering lethal doses and rapidly producing toxicity at various stages of the insect's life cycle (Esmaeilnejad et al., 2018). Studies have indicated that the superiority of silver nanoparticles over other nanosized metal particles might give them anti-insect properties (Norouzi et al., 2019).

The establishment of biological control methods employing entomopathogenic fungi (EF) has demonstrated encouraging results as a realistic alternative for the use of chemical pesticides, since they result in high mortality rates for economically significant insect pests (Mweke et al., 2018). EFs are useful as mycopesticides for insects, ticks, mites, and other arthropods of economic, medical, and veterinary significance. The potential of fungal pathogens to suppress the pest was reported by Akutse et al. (2020), who further identified three strains of *Metarhizium anisopliae* as promising biopesticides that cause mortality rates of 95.0, 87.5, and 86.3% against the adult stage of *Tuta absoluta*. Moreover, *Beauveria bassiana*, *Trichoderma asperellum*, and *Hypocrea lixii* are three EFs that have the potential of becoming endophytic fungal-based biopesticides for the control of *T. absoluta* (Agbessenou et al., 2020). Proteases, chitinases, and lipases are among the enzymes produced by entomopathogenic fungi that break down the proteins, lipids, and chitin that constitute up the host's cuticle, making it easier for hyphal penetration. Furthermore, certain EF species can produce poisonous substances such as destruxin, beauvericin, acids (dipicolinic acid and oxalic acid), lactone compounds (cepharosporolides), bassianolide terpenes (trichocaranes and fumosorinone), and others (Wang et al., 2021; Sharma et al., 2023). Noteworthy is the fact that entomopathogenic fungi that are isolated regionally are more suited to the local environment (Zeina and Laing, 2022). Consequently, obtaining novel, locally occurring isolates is crucial, especially from insect destinations. The development of efficient biocontrol agents for these insects' native species depends on these isolates. Most likely, it has been observed that *M. anisopliae*, *B. bassiana* are both effective against *T. absoluta* (Tadele and Emana, 2017; Alikhani et al., 2019).

Silver nanoparticles, synthesized with algal materials, are considered to be an emerging field of agriculture for their eco-friendly and outstanding insecticidal attributes. In addition, the interaction effects of biosynthesized AgNPs with EFs against *T. absoluta* have not been studied globally. Therefore, the present study aimed to bio-fabricate silver nanoparticles by the brown alga, *Sargassum muticum*, isolate and identify the fungus *Trichoderma harzianum* T1 from soil, evaluate the biocontrol potential of *S. muticum*-AgNPs and fungal species, both alone and in combinations, against the tomato leaf miner.

MATERIALS AND METHODS

Materials

The brown alga, *Sargassum muticum* (Pheophycophyacea) fresh seaweed was collected in polythene bags from the Red Sea coast of Jeddah, Saudi Arabia, and brought to the lab. In this study, all the reagents and chemicals related to silver nanoparticles preparation, fungi isolation, and GC-MS analysis of fungi were of analytical grade and utilized without extra purification. Distilled deionized water was used throughout the experiments whenever it is needed. These materials were purchased from Sigma-Aldrich (Missouri, USA). Reagents used for molecular identification of fungi were procured from Qiagen (Hilden, Germany).

Silver nanoparticles (AgNPs)

Preparation of extract from *S. muticum* alga

As described by (Algotiml et al., 2022), the collected seaweed was rinsed in freshwater to remove impurities. Then, the attached organisms, dust, and epiphytes were brushed off and the alga was dried in the shade for a week at room temperature after being cleaned twice with distilled water. With an electric blender (Conair™7011G, Thermo Fisher Scientific, Massachusetts, USA), the dried seaweed was chopped into a fine powder, sieved (> 0.5 mm), and stored until needed at 4 °C. The aqueous extract was prepared by heating 200 ml of deionized distilled water with 10 g of algal powder to 70 °C for 15 min. Whatman paper No. 1 was used to filter the algal precipitates three times until a clear extract was obtained. A part of the clear extract was lyophilized to use further in extract characterization, another part was kept at 4 °C till usage in nanoparticles synthesis.

Synthesis of AgNPs

The algal *S. muticum* extract was used to biosynthesize silver nanoparticles (AgNPs) according to the procedure of (Algotiml et al., 2022). In brief, 20 ml of algal extract was placed inside a conical flask together with 80 ml of a 10^{-3} M silver nitrate ($AgNO_3$, Sigma Aldrich) solution. To decrease the metal ions, the mixture was agitated on a hot plate at 70 °C for 15 min in a heating mantle. One millilitre of fresh sodium borohydride (0.03783 g 10 ml^{-1} H_2O) was added to catalyse the reduction reaction. After that, the biosynthesized AgNP solutions were cooled, carefully mixed, and kept at room temperature until use in subsequent examinations.

AgNPs characterization

Thermo-scientific Evolution 220 Spectrophotometer was used to measure the ultraviolet-visible spectra of the biosynthesized AgNPs capped by algal extract. The absorption spectra were found to be between 200 and 900 nm. To investigate the distributions, shapes, and sizes of the nanoparticles, the JEOL JEM-1100 microscope (JEOL Ltd., Tokyo, Japan) was used. After using an ultrasonicator to disperse the nanoparticles in the solution for approximately five minutes, the suspension droplet was placed on the copper grid and allowed to dry at room temperature in order to obtain Transmission Electron Microscope (TEM) measurements with a homogeneous distribution of colloidal nanoparticles on a copper grid (El Kassas and Attia, 2014). A disk of 50 mg KBr mixed with 2% finely dried specimens was prepared for the purpose of detecting the functional groups involved in AgNPs synthesized from seaweed extract. Next, a Fourier Transform Infrared Spectrometer (FTIR, Jasco Model 300E) was used to examine the disk (Verma et al., 2014). To locate relevant functional groups involved in capping and reducing the extract's biomolecules, the spectra of seaweed extract and biosynthesized AgNPs were examined in the wavenumber range of 500 to 4000 cm^{-1}. The zeta potential was determined by laser Doppler electrophoresis method. The laser diffraction of nanoparticles was recorded by Zetasizer Nano Series ZS (MAL1118778), (ELS) (Al-Zahrani et al., 2021). In order to analyze the particles using energy-dispersive X-ray spectroscopy (EDX), they were dried on a copper grid covered with carbon and then placed on a SEM device equipped with a thermal EDaX attachment. Three months following AgNPs preparation, their stability was confirmed by comparable spectra at room temperature. The absence of microbiological contamination in the AgNPs solution was verified by tests conducted on nutrient agar plates. For further studies, the AgNPs were diluted with distilled water to obtain concentrations of 2.5, 5, 10, 20, and 40 μg/ml.

Entomopathogenic fungi (EPF)

Trichoderma isolation

Trichoderma strains were isolated using the dilution plate method (Hassan and El-Awady, 2011) from soil samples taken from the rhizosphere of healthy potato plants in the Abha governorate of the West-North region of Saudi Arabia. The grown fungi were cultivated in pure culture on Potato Dextrose Agar (PDA) slants for further identification. These strains' stock cultures were deep-frozen in glycerol at -80 °C until they were needed.

DNA extraction

For DNA extraction, *Trichoderma* mycelia were cultivated for five days after being inoculated into Potato Dextrose Broth (PDB). Following that, each

Trichoderma strain's genomic DNA was extracted using a DNeasy® Plant Mini Kit (Qiagen, Hilden, Germany) in accordance with the manufacturer's instructions.

Trichoderma identification

Based on (Hassan et al., 2019), the internal transcribed spacer 1 and 2 (ITS1 and ITS2) regions of the ribosomal RNA gene cluster sequences were used to identify the strain. All of the sequences obtained by PCR, and Macrogen Co. in South Korea used a 3130 Genetic Analyzer (Applied Biosystems, Waltham, MA, USA) to perform direct amplicon sequencing from the 5′ and 3′ ends. To find homology between the PCR fragments and sequences in the GenBank database, the nucleotide BLAST software was used to compare the sequencing data with the GenBank database (http://www.ncbi.nlm.nih.gov/BLAST/). The sequences were added to the GenBank database of the National Center for Biotechnology Information (NCBI) with accession number PV335541.

Production and collection of *Trichoderma* conidia

Ten milliliters of solid Sabouraud's Dextrose Agar (SDA) medium (40 g dextrose, 10 g agar, 10 g peptone, and 60 mg CTAB/l) were placed on a 60 mm petri dish centered with a 10 mm actively growing pure culture of *T. harzianum* T1 (Senthamizhlselvan et al., 2010). The inoculation plates were incubated for seven days at 28 °C. Following the addition of 10 ml of sterile Tween 80 (0.05%) to the dishes, the isolates' conidial suspension was made using sterile glass rods to softly scrape the agar surface. Then, the suspension was gathered in 250 mL sterile beakers. After adjusting the suspension to 50 mL and separating and dispersing the conidia with a hand mixer, a hemocytometer was used to determine the conidial density, which was 1.5×10^{9} conidia per mL (Zhang et al., 2014). Dilutions were carried out by adding 10 mL of the conidial suspension to the required amount of sterile distilled water, resulting in the final concentrations of 1.5×10^{4}, 1.5×10^{5}, 1.5×10^{6}, 1.5×10^{7}, and 1.5×10^{8} conidia per ml for the fungal isolate. Before preparing the suspension, the viability of the conidia was assessed using a germination test in liquid CDB with 1% (w/v) yeast extract medium (CDBYEM) to harvest the conidia, and the conidial viability exceeded 97% for the fungal isolate.

Extraction of spore-free filtrate

The fungus was used to obtain the spore-free culture filtrate using the following procedures. The fungus was first transferred from SDA plates to flasks filled with media made of PDB. The fungal isolate was grown separately in flasks and kept for seven days at 25 °C without light in a shaker incubator. The flasks were shaken at 130 rpm to promote metabolite synthesis and fungal growth. For 15 min, the fungal broth culture was centrifuged at 4,000 rpm and -4 °C after being

incubated for seven days. This process made it easier to extract the mycelia and fungal cells from the growing media. To eliminate of any remaining debris or large particles, Whatman No. 1 paper was then used to gently filter the supernatant. Fungal metabolites free of spores were obtained by filtering the purified fungal culture via syringe-driven filters with a pore size of 0.45 m. Any remaining spores in the culture were efficiently removed during this filtering step, producing spore-free culture filtration. The purpose of this procedure was to create a pure culture free of fungus spores (Wadaan et al., 2023). To confirm the spore-free culture's purity, SDA plates were re-injected with each culture filtrate. After that, these plates were incubated at 25 °C for five days. The absence of fungal colonies on the plates following the incubation period demonstrated the actual purity of the spore-free culture. Fungal cultures that were 100 % spore-free were utilized to prepare the various concentrations by adding distilled water to be adjusted at 5, 10, 20, 40, and 60 % fungal filtrates.

Gas chromatography-mass spectrometry (GC-MS) analysis of fungal filtrate

The chemical components of the fungal isolate's filtrate were identified utilizing an Agilent Model 7890A-5975B GC-MS [Column, DB 5 ms, Agilent form (0.25 µm x 250 µm x 30 m)]. Initially the column remained at 40 °C for two min. Next, it was raised to 50 °C at an interval of 4 °C per min and held for three min. Afterwards, it was raised to 150 °C at a rate of 10 °C per min and maintained for three min. Subsequently it was raised to 220 °C at (10 °C/min) and held for six min. Lastly, it was raised to 280 °C at a rate of 15 °C per min and held for ten min. The carrier gas used in this column was pure Helium (99.999 %) for 10.9 min with a flow rate of 0.5 ml/min, then 1 ml/min per min to 1 ml/min for 30 min. Neither internal nor external chemical standards were used in this chromatographic analysis. To identify the chemical components of fungal filtrates, the mass spectrum data for each chromatograph peak were analyzed using a computerized library-searching tool (Willey 9 and NIST library).

Insects

For the establishment of a *Tuta absoluta* colony to be used in the bioassays, infested tomato leaves were collected from plants grown in unsprayed farm, kept in plastic boxes measuring 20 × 20 cm and transported to the Entomology laboratory. Infested leaves were positioned above healthy one-month-old potted tomato plants (cv. Super Strain B) on a plastic mesh with a hole width of 2 cm that was suspended from the roof of an insect rearing polyvinyl chloride cage measuring 60 × 60 × 80 cm. According to Erasmus et al. (2021) rearing method, this enabled the larvae to go from the sampled leaves onto the potted tomato plants to allow them completing their life cycle. When *T. absoluta* moths appeared, they were moved to oviposition cages with four potted healthy tomato plants (80 × 80 × 80 cm) for adult mass-rearing and were allowed to lay eggs. Adults were nutrituned with 10%

honey solution that was placed on the upper edge of each cage (Agbessenou et al., 2020). Plants were removed every two days and transferred to the other cages measuring 60 × 60 × 80 cm to confirm that the eggs that were collected from these plants were identical in age and would hatch around the same time. Three days after the larvae hatched, the leaves holding the larvae were taken off the plants and put in clear plastic containers with ventilation (20 × 20 × 7 cm) packed with tissue paper to absorb any extra moisture. Until pupation, new tomato leaves were fed to the larvae every day. Using a fine camel hair brush, the pupae were removed from the plastic containers and put into a new plastic container to emerge as adults. The oviposition and rearing cages were kept at a photoperiod of 14:10 h L:D, 65% relative humidity, and 27 ± 1 °C. Mass rearing of *T. absoluta* colony was rejuvenated every three months for several generations prior to bioassays as described above.

Bioassays

Insecticidal activity of biosynthesized AgNPs against *T. absoluta*

The efficacy of algal-biosynthesized AgNPs against larvae and pupae of the tomato leaf miner was evaluated in 24-well plates (surface area/well: 3.14 cm^2, Greiner Bio-One CELLSTAR, Vilvorde, Belgium). The third-instar larvae were carefully taken out from their mines by using zero brush as well as the newly emerged pupae were collected from soil of previously cultured infested tomato plants. Ten healthy larvae or pupae per replication/concentration (n=50) were transferred to cheesecloth and dipped into five concentrations (10 ml) of AgNPs (2.5, 5, 10, 20, and 40 µg/ml) for 5 s. They were then dropped on two paper towel sheets to absorb the excess liquid. Afterward, one larva was transferred to each well lined with 2 moistened circular filter papers (diameter = 13 mm), whereas pupa was added to well filled with 5 g moistened sterile sandy soil. Control insects were only dipped in sterilized distilled water, and then transferred individually into a well. The trays were closed with the lid, arranged with five replications in a completely randomized design (CRD); ten wells were used for each replication, representing either the control or the concentration of AgNPs. All plates were incubated in a growth chamber for 3 days at 25±2 °C in dark. Dead insects were recognized 24, 48, and 72 h after the AgNPs treatment by having no response to camel's hair brush tip probing or stereoscopic light (Van Damme et al., 2016). Corrected mortality (CM) percentages were determined using the Schneider-Orellis formula to precisely evaluate the insecticidal effect while taking the control groups' natural mortality into consideration (Puntener, 1981) as follows:

$$CM\ (\%) = \left(\frac{\%\ MT - \%\ MC}{100 - \%\ MC} \right) \times 100$$

Where MT: Mortality in Treatment, MC: Mortality in Control

LC_{50} and LC_{90} values, which represent the concentrations of the lethal substance needed to induce mortality in 50% and 90% of the exposed population, respectively, are used to assess the effectiveness of a toxic agent. The corrected mortality data's regression analysis provided these values. The computation is usually carried out using the Probit method, which reliably and precisely estimates lethal concentrations by converting mortality percentages into a linear relationship (Finney, 2004).

Fungal activity against *T. absoluta*

The same procedure was followed for bioassays with fungal conidia suspension of EPF, *T. harzianum* T1 and its spore-free liquid filtrate against larvae and pupae of *T. absoluta*. Conidial suspension of EPF was applied at 1.5×10^4, 1.5×10^5, 1.5×10^6, 1.5×10^7, and 1.5×10^8 conidia per ml, whereas fungal filtrate was used at 5, 10, 20, 40, and 60 %.

Synergistic effect of AgNPs and fungal conidia/filtrate on *T. absoluta* larvae

To evaluate the efficacy of the *S. muticum*-biosynthesized AgNPs integrated with either fungal conidial or filtrate suspensions, tomato leaves infested with third instar larvae of the moth were employed in the leaf-petri plate trial as described by El Aimani et al. (2021) with little modification. Lethal concentrations (LC_{50}) of AgNPs (42.7 µg/ml), conidial suspension (1.03×10^7 conidia/ml), and filtrate (55.7%) that have been calculated from the previous experiments were applied for single or dual treatments in this experiment. In brief, young tomato infested leaves (cv. Super Strain B) were collected from the infested-cultured plants as previously mentioned. The number of larvae per leaf was recorded, ranging from one to five. In combined treatments, each infested leaf was first immersed in the AgNPs solution (10 ml) for 5 s, it was then dipped in the 10 ml solution of fungal conidia or filtrate for another 5 s, or it was immersed in fungal conidia for 5 s then fungal filtrate for another 5 s, whereas in the individual applications, leaves were dipped in each treatment for only 5 s. The leaves were then dropped on two paper towel sheets to absorb the excess liquid, however, the leaves that serve as controls were only immersed in sterilized distilled water. Each treated leaf was transferred in a filter paper-lined Petri dish with a diameter of 9 cm with the leaf's edge in contact with wet cotton to prevent bursting, sealed with parafilm to keep *T. absoluta* larvae from escaping and stored at 25±2 °C. *T. absoluta* larval mortality (inside or outside of the leaf mines) was recorded and verified 72 h after the application as mentioned before in topic 2.5.1. For each treatment, the experimental set consisted of 10 replicate plates and repeated twice.

Statistical analysis

The SPSS software (Version 23) was used to assess the data for normality before statistical analysis by the square root transformation. The effects of three factors of substance, concentration, and exposure time were subjected to tri-factorial ANOVA using COSTAT (Version 6.400) program, with a significance level of $p < 0.05$. The means were separated using Duncan's multiple range (DMR) test.

RESULTS AND DISCUSSION

Characterization of AgNPs

UV–vis spectroscopy

After 48 h, there was a noticeable change in the reaction mixture's color from brownish to yellow due to the reduction of $AgNO_3$ by *S. muticum*. The incubation time was directly related to the brown color's intensity (**Fig. 1A**). The **Fig. 1B** displayed the UV–vis spectrum of AgNPs produced by the *S. muticum* alga extract. AgNPs absorption peaks capped by alga appeared at 407 nm. The surface plasmonic band resonance (SPR) is this peak, which is broad and less apparent because of the samples' polydispersity (Murugesan et al., 2015). The wavelength of absorbed light is strongly influenced by the size and aspect ratio of NPs. Different hues are developed by the changes in particle size in the solutions. A particular light wavelength causes the conduction electrons on the surface of the nanoparticle to vibrate, creating a variety of vivid colors. Depending on the size and structure of the particles, these vibrations result in incredibly bright hues (Al-Rubaye et al., 2020). This also is may be due to the change chemical structures which mean it has a more functional group (sterol, cholestrol, fucosterol, polar fractions, volatile fractions, aromatic esters, terpenoids, fatty acid, benzyl alcohol, benzyl dehydepremdnated, phenols, and sulfur containing compounds) (Kamenarska et al., 2002). This functional group allowed to may increase the particles size during AgNPs formation. To the AgNPs these functional groups the lower wavelength to the AgNPs capped by *Laurncia nangii* prepared at 410 nm the functional groups (poly saccharides, ß-d-galactose, galactans, pyruvic acid, complex sulfated agarans) (Kamada and Vairappan, 2012). The difference between our results and the results above studied is due to of a different study area and the collection of sampling season.

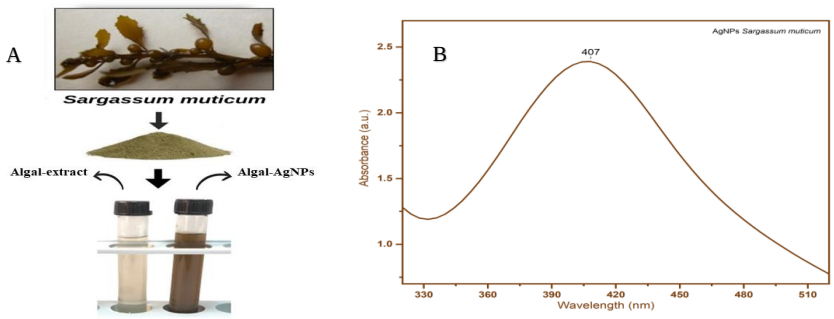

Figure 1. AgNP biosynthesis employing *S. muticum* marine algal extract as a capping and reducing agent. The reaction mixture's color changed to a brownish-yellow, indicating that the algal extract had reduced $AgNO_3$ after 48 h (A). UV-vis spectra of the biosynthesized AgNPs capped by *S. muticum* (B).

TEM analysis

Fig. 2A displays the TEM image of AgNPs capped by *S. muticum*. It can observe that the AgNPs was formed a dark point with spherical in shape, oval and hexagonal. The average particle size of 11 nm was estimated from the opposite Gaussian distribution of **Fig. 2B**.

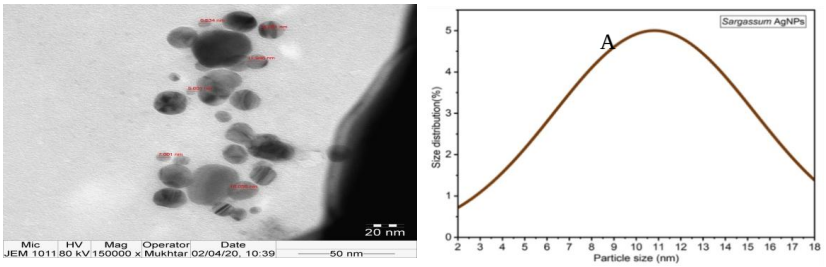

Figure 2. TEM image (A) and particle distribution (B) of AgNPs capped by *S. muticum*.

FTIR analysis

The functional groups present in the wavenumber range (4000 cm^{-1} - 400 cm^{-1}) are identified by using FTIR spectroscopy to investigate the surface chemistry of AgNPs and the *S. muticum* extract (**Fig. 3**). The spectrum of *S. muticum* aqueous extract was illustrated in **Fig. 3A**. It was found that the absorbance band at about

3440 cm^{-1} is represents the stretching vibration of the hydroxyl group in water molecule that absorbed from the air during measurement the sample and the hydroxyl group in the chemical structure carbohydrate, lipid, protein and sterol. The N-H stretching vibration in the protein of structure of *S. muticum* explains the band at about 3275 cm^{-1}. At 2927 cm^{-1} and 2857 cm^{-1}, the two peaks correspond to symmetric and asymmetric stretching vibrations of (CH_2) in carbohydrate and cholesterol, methylene cholesterol in the structure of *S. muticum*. The peak at about 1750 cm^{-1} corresponding to (C=C) stretching vibration in all content group except carbohydrate for structure in *S. muticum*. The band's clarification at about 1640 cm^{-1} is interpreted to the (C=O) in carbohydrate, lipid, protein. The peak at 1456 cm^{-1} is discus the stretching vibrations of (C-O-) and (C-C). These two groups are found in the structure of *S. muticum*. The band at about 1036 cm^{-1} is determined the rocking bending vibrations CH_3 in cholesterol. The bands at 636 cm^{-1} is characteristic the structure of (C-H) in the structure of alga. The chemical content of *S. muticum* was previously interpreted (Hamdy and Dawes, 1988). The infrared of *S. muticum*-AgNPs was discussed by comparing their spectra with the spectra of *S. muticum* extract. It was shown that absorption band appeared at 3440 cm^{-1}, for the *S. muticum* extract was shifted to higher and lower wavenumbers show in **Fig. 3B** at 3426 cm^{-1}, to AgNPs capped by *S. muticum*. The shift in Pheophycophyacea may be owing to the change of the structure after AgNPs sterilized. The absorption bands appear at 3275 cm^{-1} of *S. muticum*, for N-H stretching vibrations was shifted to higher and lower wavenumber of AgNPs surrounding by *S. muticum* at 3250 cm^{-1}. This change in frequency can be explained by the electrostatic or chemical coordination between the AgNPs and nitrogen atom in N-H group. The band at 1640 cm^{-1}, that was recommended to C=O in structure of different genera of Pheophycophyacea turned to higher and lower wavenumber at 1634 cm^{-1} in the alga. This alteration in the number of AgNPs and oxygen atom electrostatic interactions in C=O. This is because the AgNPs may be coordinate with be atom in P=O, which is explained by C-O bending vibrations. According to **Fig. 3B**, the AgNPs capped by *S. muticum* were approximately 1413 cm^{-1}. The bands at 1036 cm^{-1} that was represented to (CH_2) bending vibrations group of Pheophycophyacea genera during the addition of AgNPs assigned 1053 cm^{-1}. The band at 811 cm^{-1} of the *S. muticum* shifted at 884 cm^{-1} in AgNPs capped by *S. muticum*. This change in the band positions is due to the effect of AgNPs coordinated with N, O, P, and S which affect all chemical structure of *S. muticum*. The chemical groups of structure for different genera of Pheophycophyacea may be involved in metal complexation. The results of the present study on *S. muticum* are consistent with the results obtained by (Azizi et al., 2013).

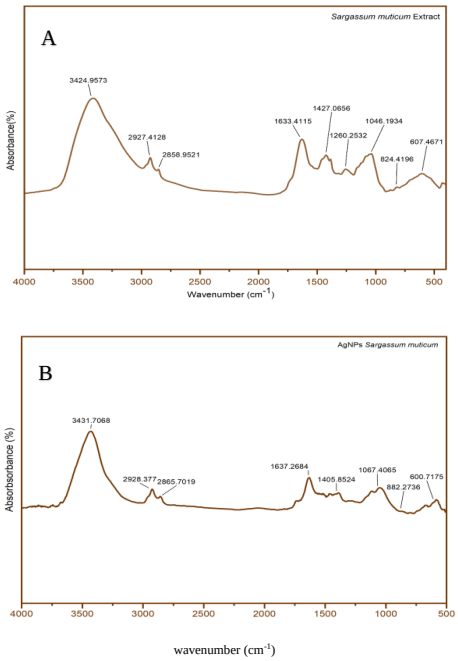

Figure 3. FTIR spectra of *S. muticum* aqueous extract (A) and biosynthesized AgNPs capped by *S. muticum* (B).

Zeta analysis

The electrical potential created at the solid-liquid interface as a result of the relative movement of the solvent and the nanoparticle is known as the zeta-potential. The manufactured silver nanoparticles were dissolved in double-distilled water to investigate the zeta potential. It is important to understand surface charge and electrical potential since they affect the stability of nanoparticles. When the zeta potential increases, it increases as well the surface potential of charged particle. **Fig. 4** demonstrates that the produced silver nanoparticle's zeta potential is -20.6 mV. These outcomes are consistent with those previously documented by several researchers on *Chaetomorpha* algae (Renuka et al., 2020; Nagasundari et al., 2021). The measured negative zeta potential affirms the presence of electrically stabilized AgNPs, and thus, the nanoparticles tend to be more within the suspension. In general, zeta potential stability ranges between -20 and 30 mV. Similarly, *C. antennina*-Ag nanoparticles with a zeta potential value of -27.4 mV exhibited

similar results (Kingslin et al., 2022). This suggests that SNPs are extremely stable; this could be because of the stronger attraction and repelling force that exists between nanoparticles. Moreover, ELS analysis of *Chaetomorpha ligustica*-AgNPs showed the zeta potential of 2.36 mV indicating aggregation of nanoparticles (Al-Zahrani et al., 2021). Because the bioactive ingredients in the seaweed extract might have been adsorbed to the surface of the synthesized nanoparticles, a negative surface charge was detected. If the zeta potentials of the particles in suspension are significantly negative or positive, respectively, they will be more likely to reject one another and less likely to combine (Tavakol et al., 2017). Stable synthesized nanoparticles are defined by achieving zeta potential values greater than −20 mV or more than +20 mV. According to a previous study (Fatima et al., 2020), elements with a zeta balance potential of ± 30 mV have difficulty aggregating nanoparticles due to electron-fixed revulsion. The surface charge of the biosynthesized Cp-AgNPs was -35.2 mV, indicating that they were highly stable by electrostatic mean (Viswanathan et al., 2024).

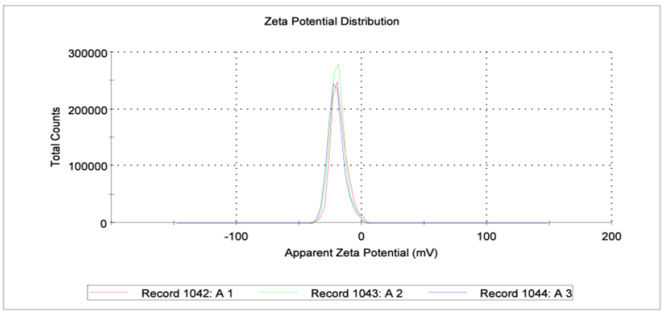

Count rate (kcps)	Z-Potential (mV)	Mean (mV)	Area (%)	St. Dev. (mV)	Z- Deviation (mV)	Conductivity (mS/cm)
206.3	-20.6	-20.6	100.0	6.48	6.48	1.01

Figure 4. Characterization of biologically synthesized *S. muticum*-AgNPs using zeta potential distribution – ELS.

EDX analysis

The basis of pure AgNPs may be identified in the energy-dispersive X-ray spectroscopy profile of the biosynthesized *S. muticum*-AgNPs powder if it shows strong Ag signals in contrast to loose carbon peaks (**Fig. 5**). Additionally, the presence of Ag, C, O2, k, Cl, S, Si, Mg, and Na compounds in examined samples is authorized by visible peaks. According to the surface plasmon-resistance, an intense signal was detected at 2.983 KeV, revealing that Ag was the predominant

element, accounting for approximately 9.08% of mass. These findings are agreed with the results of (Khan et al., 2013; Rajivgandhi et al., 2020).

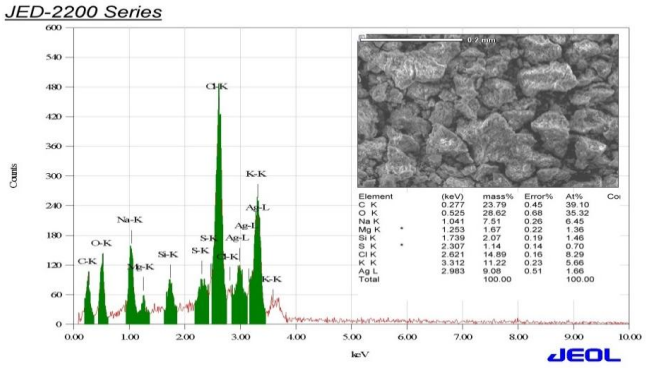

Figure 5. EDX of biosynthesized *S. muticum*-silver nanoparticles.

Identification of the fungus

After the ITS regions were amplified in several strains, PCR products totaling roughly 600 base pairs (bp) were immediately sequenced. BLAST analysis was performed on the sequences in comparison to the NCBI database. We identified the strains as *T. harzianum* T1 (**Fig. 6A**). The similarity among *T. harzianum* T1, *T. harzianum* MF780850 and *T. afroharzianum* MT102402 was ranged from 99 and 100%. Applying MEGA 5.1 software, the phylogenetic tree was created with the nucleotide sequences of the eight *Trichoderma* strains' cloned ITS regions. There were two different phylogenetic sub-clades formed by the strains (**Fig. 6B**). Isolates of *T. harzianum* T1, *T. harzianum* MF780850, and *T. afroharzianum* MT102402 were included in Group 1 with about 100% similarity; it included also, *T. aureoviride* MZ769130, *T. virens* LT707586 and *T. longibrachiatum* OP710044. The second main clade included *T. koningiopsis* KP340272 and *T. asperellum* MH259829 with about 65% similarity. A significant phylogenetic space of almost 100% was found when the nucleotide sequences of all ITS fragments were subjected to joint phylogenetic analysis. As a result, the seven species were distinguished from each other by the ITS analysis. Similar to this, Kuhls et al. (1997) differentiated between *T. reesei* and *T. longibrachiatum* via sequence analysis. Other researchers have identified *T. harzianum* using ITS sequences (Fahmi et al., 2016). Several *Trichoderma* species' ITS sequences were aligned multiple times, indicating nucleotide sequence differences that might be used to separate between them (Hassan et al., 2019). The genus *Trichoderma* is commonly found as

wood-decomposing or soil-borne fungi. Certain species are commercially significant due to their production of industrial enzymes (chitinase, cellulase, and hemicellulase), biocontrol agents and antibiotics (Hassan, 2014; Fahmi et al., 2016).

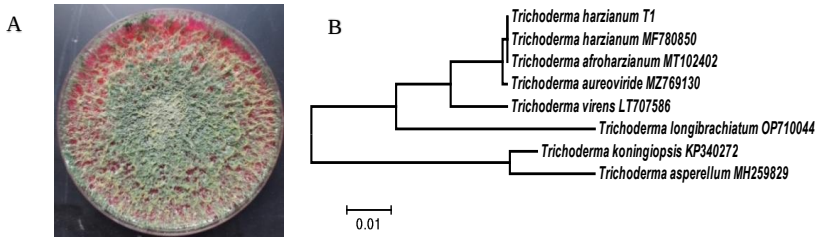

Figure 6. *T. harzianum* T1 growing on SDA medium 7 days after inoculation (a). The GenBank database's neighbor-joining tree displays the genetic diversity of the *T. harzianum* strain together with associated sequences of a few similar fungal strains based on the sequence analysis of the ITS region (b).

GC-MS analysis of fungal filtrate

In this study, GC-MS analysis was performed on the filtrate of the target fungal isolate. Ten different chemical substances were identified in the fungal filtrate (**Table 1**). The results showed that *T. harzianum* T1 contained the most bioactive substance with large amount, which was 6,8-dibromo-2-(3-pyridyl)-4-phenyl-quinazoline representing 70.31% at retention time 42.4 min. The other main abundantly constituents were 3',4'-dihydro-2'-(morpholin-4-yl)-5',7'-dinitrospir o[cyclopentane-1,3'-quinazoline] (5.98%) at 18.8 min, Docosane (5.46%) at 14.8 min, 3-Ethyl-5-(2-ethylbutyl)octadecane (4.71%) at 19.5 min, and Palmitic acid (4.29%) at 22.8 min. On the other hand, a small amount of Boric acid, ethyl-, didecyl ester (1.93%), Eicosane (1.57%), and Phytane (0.45%) have been detected. The compounds found in the filtrate of the fungal isolate *T. harzianum* T1 were classified as belonging to the following groups: ketones, chlorinated hydrocarbon, carboxylic acid, heterocyclic amine, aromatic hydrocarbon, aliphatic hydrocarbon, alkaloid, fatty acid, and alkane hydrocarbon. Many heterocyclic compounds with nitrogen as quinazolinone derivatives have been shown to possess a broad range of biological activity. In the current investigation, high percentage of the bioactive compound 6,8-dibromo-2-(3-pyridyl)-4-phenyl-quinazoline was detected in *T. harzianum* filtrate which had nematicidal, insecticidal, and antimicrobial properties (Zheng et al., 2012; Baazeem et al., 2022). Although the biological activity of fungal filtrates is typically caused by major components, the impact of minor ones cannot be ignored. Our findings were also confirmed with the record of Oliveira et al. (2009) who reported that many

nematode species are known to be extremely killed by palmitic acid. Other compounds with minor content were Boric acid, ethyl-, didecyl ester, Eicosane, and Phytane that had been classified as keto acid and alkanes, respectively and have been used as biocides (Bhat et al., 2024; Wang et al., 2024).

Table 1. GC-MS analysis of the filtrate of *T. harzianum* T1.

Active compounds	Rt. (min)	Relative Content (%)
2-Methylhexacosane	22.2	2.35
3',4'-dihydro-2'-(morpholin-4-yl)-5',7'-dinitrospiro[cyclopentane-1,3'-quinazoline]	18.8	5.98
3-Ethyl-5-(2-ethylbutyl)octadecane	19.5	4.71
6,8-dibromo-2-(3-pyridyl)-4-phenyl-quinazoline	42.4	70.31
9-n-Butyldocosane	15.7	2.95
Boric acid, ethyl-, didecyl ester	21.6	1.93
Docosane	14.8	5.46
Eicosane	24.0	1.57
Palmitic acid	22.8	4.29
Phytane	21.7	0.45

Rt. = Retention time.

Insecticidal activity

Biosynthesized-AgNPs

The toxicity of *S. muticum*-AgNPs to *T. absoluta* larvae and pupae was investigated (**Fig. 7, Table 2**). Significant differences ($p < 0.05$) observed in the mortality % of *T. absoluta* larvae throughout exposure times and *S. muticum*-AgNP concentrations (**Fig. 7A**). Corrected mortality percentages of caterpillars ranging from 2.0 to 46.0% were recorded 24 h post treatment. The mortality rates from the different alga-AgNP concentrations after two days ranged from 8.8 to 57.2%. *S. muticum*-AgNPs attained 64.8% mortality at the maximum concentration (40 µg/ml) on the third day of the experiment. Nevertheless, 17.2%, 24.8%, 31.2%, and 51.2% mortality percentages were recorded with 2.5, 5, 10, and 20 µg/ml concentrations, respectively (**Fig. 7A**). The toxicity of *S. muticum*-AgNPs against *T. absoluta* pupae was considerable (**Fig. 7B**). Pupal mortality rates after applying nanoparticles for 24 h varied from 0.0 to 23.2%. While the highest concentration (40 µg/ml) and lowest concentration (2.5 µg/ml)

resulted in mortality percentages of 39.6% and 5.2%, respectively, 72 h-post application. The 95% confidence intervals of the mortality percentage showed a significant difference ($p < 0.05$) between the calculated LC_{50} and LC_{90} values of the *S. muticum*-AgNPs (**Table 2**). The LC_{50} and LC_{90} values of the algal-AgNPs on larvae were significantly lower compared to pupae. At 72 h of exposure, the *S. muticum*-AgNPs was the most toxic against larvae and pupae with estimated LC_{50} and LC_{90} values of 25.4 and 63.6, and 45.9 and 92.7 µg/ml, respectively. At $p < 0.05$, the reactions of *T. absoluta* larvae and pupae to the nanoparticles matched the log (concentration)/probit (mortality) model (**Table 2**). With slope coefficients ranging from 1.17 to 2.27, the *S. muticum*-AgNPs appeared to respond homogeneously to the varying concentration. Since brown algae species are known to contain chemicals with biological characteristics, there is plenty of *S. muticum* material that is not currently being used but may have significant potential (Silva et al., 2024). Additionally, there is a greater search for natural resources due to the growing interest in eco-friendly materials, and *S. muticum* has been found to be a rich source of bioactive substances, particularly polyphenols with antiproliferation, antidiabetic, antioxidant, anti-inflammatory, antitumor, antimicrobial and insecticidal activities (Zheng et al., 2024; Mardani-Talaee et al., 2025). Only marine algae contain the naturally occurring seaweed polyphenolic molecules tannins and flavonoids (Li et al., 2010). The literature survey estimated that AgNP is very effective against *Liriomyza trifolii* more than *T. absoluta* and *Spodoptera litoralis* with LC_{50} averaged 7.41, 7.72 and 9.93 ppm, respectively, in laboratory, however in the field, reduction percentages were 73.5, 65.1 and 54.8% for *L. trifolii, T. absoluta* and *S. litoralis* (Marouf and Abd-Allah, 2021). Our finding meet with Zayed (2021) who indicated that chitosan nanoparticles had a potent insecticidal activity against 2nd larval instar and eggs deposited/female of *T. absoluta* whereas, chitosan hydroxyapatite nanoparticles was the highest effective treatment on antifeedant and growth inhibition. Also, Hany et al. (2016) confirmed the effectiveness of nano silica on larvae of *T. absoluta*. Our findings are consistent with the documented insecticidal properties of biogenic iron oxide nanoparticles (FeNPs) of *Ulva lactuca* against *T. absoluta* (Ramya et al., 2023).

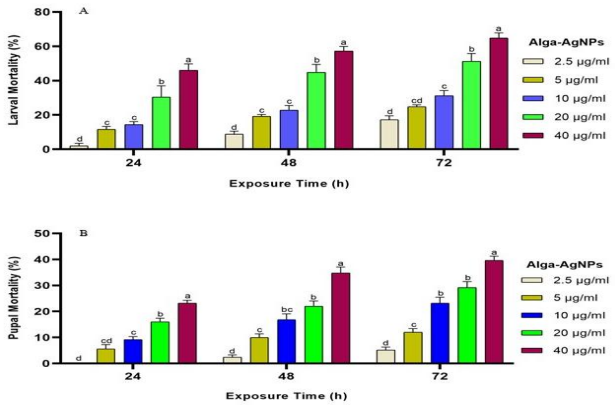

Figure 7. Insecticidal activity of *S. muticum*-AgNPs on *T. absoluta* larvae (A) and pupae (B). According to the DMR test, bars that have the same letter labeled are not statistically different ($p < 0.05$).

Table 2. LC_{50} and LC_{90} of *S. muticum*-AgNPs against *T. absoluta* larvae and pupae.

T. absoluta	Exposure Time (h)	LC_{50} (µg/ml) (95% LCL–UCL)	LC_{90} (µg/ml) (95% LCL–UCL)	Slope ± SE	Intercept	X^2	*p*-value
Larvae	24	40.8 (27.9-90.3)	74.1 (50.1-119.7)	2.27±0.15	-1.49	9.2	0.023
	48	31.2 (21.2-67.5)	67.3 (45.5-153.6)	1.36±0.11	-1.12	9.3	0.026
	72	25.4 (21.7-30.4)	63.6 (53.5-80.3)	1.87±0.12	-0.85	5.1	0.168
Pupae	24	62.2 (39.2-153.1)	107.0 (63.1-223.2)	1.55±0.15	-1.78	8.2	0.042
	48	50.9 (42.1-67.2)	95.5 (76.4-132.6)	1.29±0.13	-1.46	7.8	0.050
	72	45.9 (28.8-71.5)	92.7 (55.0-189.9)	1.17±0.14	-1.25	9.9	0.019

Lethal concentrations that kill 50 and 90 % of larvae or pupae (LC_{50}, LC_{90}), Lower confidence limit (LCL), upper confidence limit (UCL), chi-squared value (X^2), standard error (SE), and probability (*p*-value).

T. harzianum T1 fungus

The effect of treatment (conidial suspension concentrations and exposure times) significantly influenced larval and pupal mortalities ($p < 0.05$) as shown in **Fig. 8 and Table 3**. In addition, the larvae were more susceptible than the pupae to different concentrations. The mortality percentages increased with the extension of exposure time. Across all concentrations, 1.5×10^8 conidia/ml was reported to exhibit the highest mortality rate of 92.0 and 80% in larvae and pupae, respectively by 72 h (**Fig. 8**). Regarding 24 and 48 h exposure, median (1.5×10^6 conidia/ml) and lower concentrations (1.5×10^5 conidia/ml) caused not significantly different mortality percentages, ranging from 20.8 to 34.4% for larvae (**Fig. 8A**) and 18.8 to

29.6% for pupae (**Fig. 8B**). The calculated LC_{50} and LC_{90} values for fungus conidial suspension varied from lowest to highest as follows: 8.9×10^{5} to 1.6×10^{14} conidia/ml and 3.8×10^{6} to 3.7×10^{17} conidia/ml for larvae and pupae, respectively (**Table 3**). Due to the concentrations under investigation, the *T. absoluta* larvae and pupae displayed various degrees of homogeneity, with slope values ranging from 1.76 to 3.44 (**Table 3**). The data in **Fig. 9 and Table 4** represent the toxicity of fungal filtrate against *T. absoluta* larvae and pupae under laboratory conditions. As exposure time and fungal filtrate concentration increased, the percentage of larval and pupal mortalities increased dramatically ($p < 0.05$). The EPF conidial-free filtrate at higher concentration (60%) significantly affected larval and pupal mortalities ($p < 0.05$) among all three days (**Fig. 9**). At 72 h exposure, the percentage of mortality caused to larvae (70.0%) (**Fig. 9A**) was significantly higher than that caused to pupae (59.2%) (**Fig. 9B**). The lowest mortality percentages (4.0 and 2.8%) were recorded in the plates where the larvae and pupae were exposed to *T. harzianum* T1 filtrate at the rate of 5% after 24 h application. Likewise, **Table 4** shows that the fungal isolate filtrate was more potent against larvae than pupae, with LC_{50} values for the former being 63.9, 51.5, and 36.8% at 24, 48, and 72 h after treatment, and for the latter being 70.4, 63.2, and 48.1% at the same times. The same results appeared for the LC_{90} values, that were significantly lower for larvae than for pupae. In addition, the data in **Table 4** demonstrate that the *T. absoluta* larval response exhibited the highest degree of homogeneity following exposure to the filtrate, with a slope value of 2.65 at 72 h following treatment.

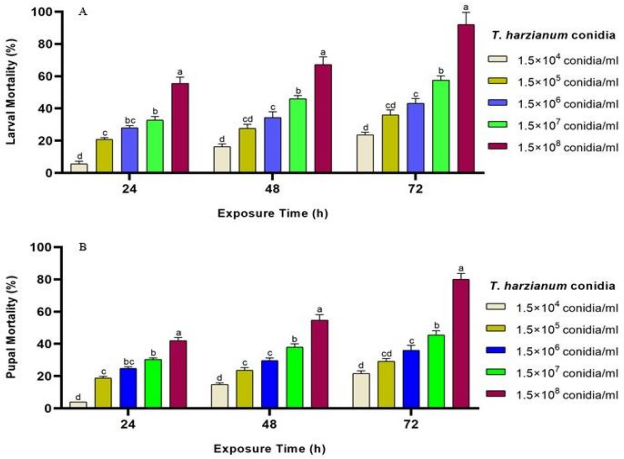

Figure 8. Corrected mortality percentages of *T. absoluta* (mean ± SE) subjected to five concentrations of *T. harzianum* T1 conidial suspension, for larvae (A) and pupae (B) after 24, 48 and 72 h. Mean values of concentrations with the same letter(s) do not differ statistically significantly according to DMR test, ($p < 0.05$).

Table 3. LC_{50} and LC_{90} of *T. harzianum* T1 conidial suspension against *T. absoluta* larvae and pupae.

T. absoluta	Exposure Time (h)	LC_{50} (conidia/ml) (95% LCL–UCL)	LC_{90} (conidia/ml) (95% LCL–UCL)	Slope ± SE	Intercept	X^2	*p*-value
Larvae	24	7.9×10^{7} (7.3-8.7)*	1.6×10^{14} (11.9-19.1)	2.63±0.11	-2.82	5.1	0.168
	48	9.5×10^{6} (6.6-7.5)	6.3×10^{10} (9.8-12.4)	2.35±0.16	-2.34	2.0	0.580
	72	8.9×10^{5} (4.5-7.4)	6.8×10^{8} (7.4-17.2)	3.44±0.13	-2.64	15.6	0.001
Pupae	24	3.3×10^{8} (7.9-9.6)	3.7×10^{17} (13.7-27.8)	2.08±0.21	-2.62	3.41	0.169
	48	9.3×10^{7} (7.3-9.3)	2.8×10^{12} (10.9-15.3)	1.76±0.15	-2.16	1.98	0.577
	72	3.8×10^{6} (5.4-9.1)	1.2×10^{10} (8.2-22.9)	2.65±0.22	-2.40	12.05	0.007

Lethal concentrations that kill 50 and 90 % of larvae or pupae (LC_{50}, LC_{90}), Lower confidence limit (LCL), upper confidence limit (UCL), chi-squared value (X^2), standard error (SE), and probability (*p*-value). * Parenthesized figures are given as powers of 10.

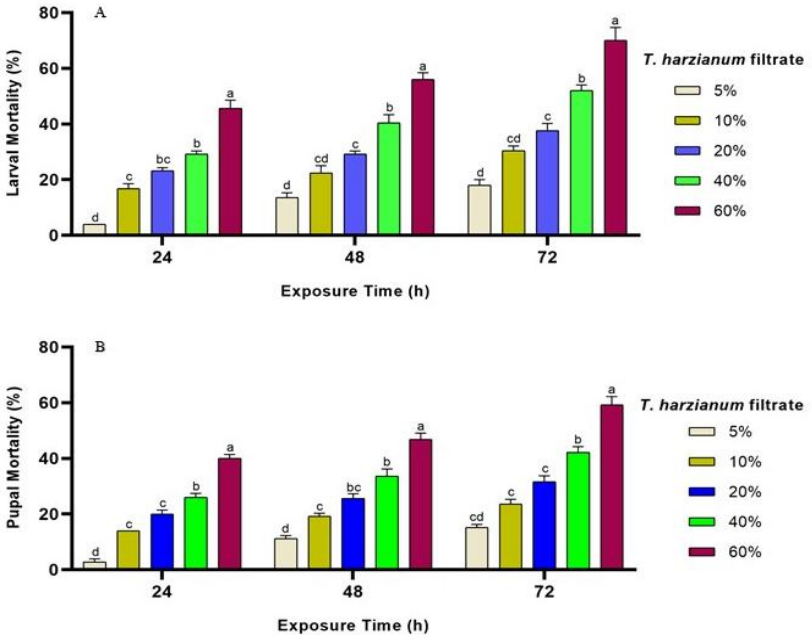

Figure 9. Percentage of larval (A) and pupal (B) mortalities of *T. absoluta* exposed for 1, 2 and 3 days to *T. harzianum* T1 filtrate. The statistical significance (DMR test, $p < 0.05$) is indicated by different letters above the bars (mean ± SE).

Table 4. LC_{50} and LC_{90} of *T. harzianum* T1 filtrate against *T. absoluta* larvae and pupae.

T. absoluta	Exposure Time (h)	LC_{50} (%) (95% LCL–UCL)	LC_{90} (%) (95% LCL–UCL)	Slope ± SE	Intercept	X^2	*p*-value
Larvae	24	63.9 (44.7-85.3)	83.2 (74.6-120.5)	2.21±0.15	-1.35	8.36	0.039
	48	51.5 (44.3-62.7)	75.4 (64.2-96.8)	2.16±0.12	-1.04	1.81	0.613
	72	36.8 (31.8-43.0)	62.4 (51.7-71.2)	2.65±0.20	-0.86	2.52	0.043
Pupae	24	70.4 (49.1-126.5)	92.8 (64.9-186.1)	1.61±0.17	-1.45	3.64	0.049
	48	63.2 (53.0-81.5)	84.7 (70.1-113.2)	1.78±0.18	-1.12	2.17	0.538
	72	48.1 (41.5-58.0)	73.7 (62.7-92.3)	1.80±0.14	-0.99	1.70	0.036

Lethal concentrations that kill 50 and 90 % of larvae or pupae (LC_{50}, LC_{90}), Lower confidence limit (LCL), upper confidence limit (UCL), chi-squared value (X^2), standard error (SE), and probability (*p*-value).

The findings of this study demonstrate that when used as an immersion solution, *T. harzianum* T1 may efficiently kill a significant percentage of *T. absoluta* larvae and pupae. This was particularly true for the conidial suspension, which not only had the lowest estimated LC_{50} and LC_{90} values against larvae and pupae but also displayed fast-acting properties by causing an approximate 86% mortality rate in larvae and pupae after three days of exposure. Mkiga et al. (2020) examined the significance of body surface availability for attachment of *Metarhizium anisopliae* conidia in females *Thaumatotibia leucotreta* (Lepidoptera: Tortricidae). The dose-responses noticed by Contreras et al. (2014), who investigated a liquid formulation of *M. anisopliae* conidia against *T. absoluta* pupae, were analogous to those reported in the current investigation. It just took a single day for conidia to germinate and pierce the larval and pupal cuticles. Thus, a faster conidial germination rate and cuticle penetrating capacity of the *T. harzianum* T1 may be responsible for the observed variations in toxicity between the conidia and filtrate (Erasmus et al., 2021). Abdel-Raheem et al. (2015) conducted laboratory bioassays and concluded that when *T. absoluta* eggs were exposed to *M. anisopliae* and *Beauveria bassiana*, there was 100% mortality at 1×10^7 conidia ml^{-1}. Similar to the obtained results, it was evident that the larval stage was extremely vulnerable to isolates of both *B. bassiana* and *M. anisopliae*, with mortalities surpassing 90% (Tadele and Emana, 2017). According to (Abebe (2019), the mortality rates of *T. absoluta* larvae in field and pot trials caused by the application of *B. bassiana* were 61.8 and 67.8%, respectively.

Synergistic effect of *S. muticum*-AgNPs and *T. harzianum* T1

As shown in **Fig. 10**, the average corrected mortality percentages for larvae of *T. absoluta* treated with separate or joint treatments for 72 h ranged from 47.6 to 96.0%. When *S. muticum*-AgNPs were used in combination with conidial

suspension, larval mortality increased significantly (96.0%, $p < 0.05$) in comparison to all other treatments. AgNPs + filtrate suspension and fungal conidia + filtrate treatments, on the other hand, killed 85.2 and 91.2% of *T. absoluta* larvae without significant differences between them. Additionally, applying fungal conidia alone caused 68% mortality, and filtrate alone recorded 56.4% that was statistically significant. By 47.6%, the least significant mortality value was obtained when *S. muticum*-AgNPs were applied alone. For the first time, this study explores, the fabrication of indigenous alga, and evaluates the separate and combined effects of the biosynthesized *S. muticum*-AgNPs with the conidia or filtrate of local *T. harzianum* T1 fungus against *T. absoluta* larvae and pupae.

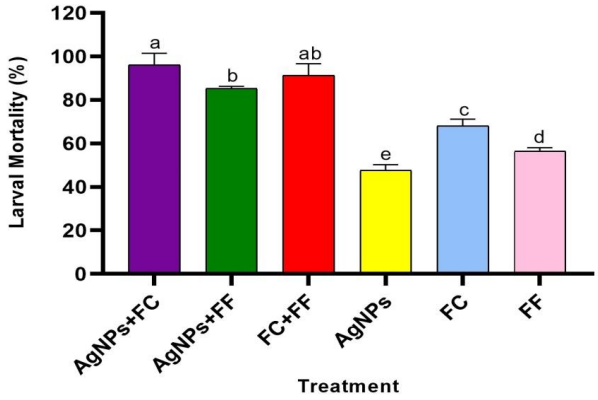

Figure 10. Percentage of larval mortality of *T. absoluta* exposed for 3 days to *S. muticum*-AgNPs integrated with either conidia or filtrate suspension of *T. harzianum* T1. FC=fungal conidia, FF=fungal filtrate. Different letters above bars (mean ± SE) indicate statistical significance (DMR test, $p < 0.05$).

Increasing biological activity against the target organism and lowering participant concentration are the two primary goals of employing synergistic combinations. Additionally, the possibility of resistance selection and the ensuing generation of resistant populations are reduced by combinations with higher chemical complexity (Kucharska et al., 2011). Extensive experiments using target host time- and concentration-dependent mortality response and toxin-pathogen compatibility are necessary to produce a stable and successful pest management strategy. This investigation definitively demonstrated that applying *T. harzianum* T1 alone or combined with *S. muticum*-AgNPs was lethal to larval and pupal stages of tomato leafminer. Moreover, the fungus was shown to be compatible with

the addition of AgNPs, and their dual application was determined to be a desirable strategy to get over the slow mortality assessment by creating a powerful additive or synergistic interaction that eventually improves the mortality of *T. absoluta*. Thus, the use of bio-synthesized AgNPs in IPM programs that also employ fungus biological control agents offers a number of important challenges, as this study demonstrate. Feng et al. (2004) demonstrated that the toxicological interaction of specific compounds with fungal candidates might result in either a decrease in toxicity (antagonism), increase toxicity additively, or the mixture's ideal toxicity increasing (synergism). Consequently, in the present work, three days following treatment, the tested EPF's interaction with AgNPs seems to have a synergistic or additive effect on *T. absoluta* mortality. *T. harzianum* T1 used here either by conidial suspensions or filtrates was able to kill larvae, when either applied individually or concomitantly. Synthesized zinc oxide nanoparticles' larvicidal action against *Culex quinquefasciatus* and *Anopheles subpictus*, showed an increase in mortality with increasing concentration; additionally, when the ideal time for ZnO nanoparticles' lethal effects was taken into consideration, it was 100 % proven after 24 h (Kirthi et al., 2011). Similarly, (Hersanti et al., 2020) found that the application of a *B. bassiana* + silica NPs 5 % + carbon fiber mixture resulted in the highest mortality rate of *Spodoptera litura* larvae (53.3 %), as versus 6.7 % mortality when *B. bassiana* was employed alone. The rapid mortality response that the fungal conidial suspensions in this investigation demonstrated is consistent with earlier research that aimed to screen the most virulent isolate against a range of pest species (Hussain, 2021). By penetrating the insect's cuticle, the *T. harzianum* can release hydrolytic enzymes known as cuticle-degrading enzymes, which include lipases, proteinases, and chitinases (Lakhdari et al., 2023). Although the insecticidal activity of the AgNPs alone was only moderately efficient in this investigation, the addition of EPF may increase their effectiveness. When individuals exposed to conidial suspension integrated with AgNPs, *T. absoluta* larvae showed higher mortality than pupae, indicating strong the sensitivity to this treatment in the current investigation. This observation may be explained by the pupae' higher chitinized cuticle area relative to the larvae's less chitinized body area. Applying *S. muticum*-AgNPs in combination with *T. harzianum* T1 promises to be more effective against insects, according to the outcomes of the current preliminary data. However, more research focusing on other economically significant insect species is required to elucidate their formulation development, adverse effects, and mode of action in order to validate the method's effectiveness.

CONCLUSIONS

There are numerous secondary metabolites generated by algae. These compounds are promising as environmentally friendly methods for preventing the serious damage that pests in agroecosystems do. Furthermore, entomopathognic fungi have been shown to be significant in protecting plants from insect attacks. Aadaptability and resistance of tomato leaf miner, *T. absoluta* to chemical insecticides have necessitated integrated pest management (IPM) strategies prioritizing sustainable alternatives.

In the present study, we successfully synthesized the AgNPs using *S. muticum* algal extract with a straight forward repeatable methodology. UV-Vis, TEM, FTIR, zeta potential, and XRD analyses were used to characterize the biosynthesized AgNPs. We also successfully isolated and molecularly identified the native fungus *T. harzianum* T1 as well as subjected the fungal filtrate to GC-MS analysis. Furthermore, the insecticidal effect of *S. muticum*-AgNPs either individually or integrated with *T. harzianum* T1 conidial/filtrate suspension against larvae and pupae of the tomato leaf miner, *T. absoluta* was evaluated, indicating that the larvicidal activity of all tested compounds was better than pupicidal activity. *S. muticum*-AgNPs together with the *T. harzianum* T1 conidial suspension has a greatest insecticidal impact on *T. absoluta* larvae which can be widely used in tomato production. This study demonstrates the suppressive ability of EPF conidia in disrupting the life cycle of *T. absoluta* for use in IPM programs, ideally in conjunction with algal-AgNPs for larval and pupal control. However, more research should be carried out on the effectiveness and durability of EPFs or other bio-agents, as well as biosynthesized nanoparticles, in both field and greenhouse settings, in soil types with various characteristics. While examining the genetic heterogeneity of *T. absoluta* responses across various geographic populations and crop varieties, it would also be pertinent to describe the lethal effects of tested components on pest growth, reproduction, and behavior. Finally, it is important to investigate how these materials affect non-target biodiversity in the environment and how various nanotechnological formulations might be developed to increase their stability and controlled release in agricultural applications.

ACKNOWLEDGMENTS

The authors extend their appreciations to Taif University, Saudi Arabia, for supporting this work through project number (TU-DSPP-2024-168).

FUNDING

This research was funded by Taif University, Saudi Arabia, Project No. (TU-DSPP-2024-168).

REFERENCES

Minchev, Z., Ramírez-Serrano, B., Dejana, L., Lee Díaz, A.S., Zitlalpopoca-Hernandez, G., Orine, D., Saha, H., Papantoniou, D., García, J.M., González-Céspedes, A., Garbeva, P., van Dam, N.M., Soler, R., Giron, D., Martínez-Medina, A., Biere, A., Hauser, T., Meyling, N.V., Rasmann, S., & Pozo, M.J. (2024). Beneficial soil fungi enhance tomato crop productivity and resistance to the leaf-mining pest *Tuta absoluta* in agronomic conditions. *Agronomy for Sustainable Development*, *44*, 1–16.

Skendžić, S., Zovko, M., Pajač Živković, I., Lešić, V., & Lemić, D. (2021). Effect of climate change on introduced and native agricultural invasive insect pests in Europe. *Insects*, *12*, 985.

Zhang, P., Min, L., Tang, J., Rafiq, M. K. & Sun, H. (2020). Sorption and degradation of imidacloprid and clothianidin in Chinese paddy soil and red soil amended with biochars. *Biochar*, *2*, 329–341.

Erasmus, R., Berg, J.V., & Plessis, H.D. (2021). Susceptibility of *Tuta absoluta* (Lepidoptera: Gelechiidae) pupae to soil applied entomopathogenic fungal biopesticides. *Insects*, *12*, 515.

Bakheit, E.H., Taha, A.K., Mahmoud, M.E., Abdelhalim, T.S., Mustafa, K.A., Mohamed, E.I., & Abdellateef, E. (2023). Prospects of resistance of some Sudanese tomato accessions to tomato fruit borer (*Tuta absoluta*) (Meyrick, 1917) (Lepidoptera: Gelechiidae) and its mechanism. *International Journal of Tropical Insect Science*, *6*, 2067–2082.

Biondi, A., Guedes, R.N.C., Wan, F-H., & Desneux, N. (2018). Ecology, worldwide spread, and management of the invasive South American tomato pinworm, *Tuta absoluta*: Past, present, and future. *Annu. Rev. Entomol.*, *63*, 239–258.

Vivekanandhan, P., Swathy, K., Alahmadi, T. A., & Ansari, M.J. (2024). Biocontrol effects of chemical molecules derived from *Beauveria bassiana* against larvae of *Tuta absoluta* (Meyrick) (Lepidoptera: Gelechiidae). *Front. Microbiol.*, *15*, 1336334.

Tarusikirwa, V.L., Machekano, H., Mutamiswa, R., Chidawanyika, F., & Nyamukondiwa, C. (2020). *Tuta absoluta* (Meyrick) (Lepidoptera: Gelechiidae) on the "Offensive" in Africa: Prospects for integrated management initiatives. *Insects*, *11*(11), 764.

Krache, F., Boualem, M., Abdellaoui, A., Ould, M.H., Benabdelmoumene, D., & Keddar, F. (2022). Effect of botanical extract of garlic (*Allium sativum* L.) on larvae of tomato leaf miner *Tuta absoluta* (Meyrick) (Lepidoptera: Gelechiidae). *Pap. Life Sci. Mar. Environ. Res.*, *1*, 6–9.

Gebremariam, G. (2015) *Tuta Absoluta*: A global looming challenge in tomato production: Review paper. *J. Biol. Agric. Health*, *5*(14), 57–63.

Abd El-Ghany, N.M., Abdel-Razek, A.S., Djelouah, K., & Moussa, A. (2018). Efficacy of bio-rational insecticides against *Tuta absoluta* (Meyrick) (Lepidoptera: Gelechiidae) on tomatoes. *Biosci. Res.*, *15*, 28–40.

Judith Vijaya, J., Jayaprakash, N., Kombaiah, K., Kaviyarasu, K., John Kennedy, L., Jothi Ramalingam, R., Al-Lohedan, H.A., Mansoor-Ali, V.M., & Maaza, M. (2017). Bioreduction potentials of dried root of *Zingiber officinale* for a simple green synthesis of silver nanoparticles: Antibacterial studies. *Journal of Photochemistry and Photobiology B: Biology*, *177*, 62–68.

Usman, M., Farooq, M., Wakeel, A., Nawaz, A., Cheema, S.A., Rehman, H., Ashraf, I., & Sanaullah, M. (2020). Nanotechnology in agriculture: Current status, challenges and future opportunities. *Science of the Total Environment*, *721*(15), 137778.

Arya, A., & Chundawat, T.S. (2018). Metal nanoparticles from algae: A green approach for the synthesis, characterization and their biological activity. *Nanosci. Nanotechnology-Asia*, *10*(2), 185–202.

Jeyarani, S., Vinita, N.M., Puja, P., Senthamilselvi, S., Devan, U., Velangani, A.J., Biruntha, M., Pugazhendhi, A., & Kumar, B. (2020). Biomimetic gold nanoparticles for its cytotoxicity and biocompatibility evidenced by fluorescence-based assays in cancer (MDA-MB-231) and non-cancerous (HEK-293) cells. *J. Photochem. Photobiol. B Biol.*, *202*, 111715.

Badineni, V., Maseed, H., Arla, S.K., Yerramala, S., Naidu, B.V.K., & Kaviyarasu, K. (2021). Effect of PVA/PVP protective agent on the formation of silver nanoparticles and its photocatalytic and antimicrobial activity. *Materials Today: Proceedings*, *36*(2), 121–125.

Valsalam, S., Agastian, P., Arasu, M.V., Al-Dhabi, N.A., Ghilan, A.M., Kaviyarasu, K., Ravindran, B., Chang, S.W., & Arokiyaraj, S. (2019). Rapid biosynthesis and characterization of silver nanoparticles from the leaf extract of *Tropaeolum majus* L. and its enhanced in-vitro antibacterial, antifungal, antioxidant and anticancer properties. *Journal of Photochemistry and Photobiology B: Biology*, *191*, 65–74.

Mani, M., Okla, M.K., Selvaraj, S., Kumar, A.R., Kumaresan, S., Muthukumaran, A., Kaviyarasu, K., El-Tayeb, M.A., Elbadawi, Y.B., Almaary, K.S., Almunqedhi, B.M.A., & Elshikh, M.S. (2021). A novel biogenic *Allium cepa* leaf mediated silver nanoparticles for antimicrobial, antioxidant, and anticancer effects on MCF-7 cell line. *Environmental Research*, *198*, 111199.

Sathiyaraj, S., Suriyakala, G., Gandhi, A.D., Babujanarthanam, R., Almaary, K.S., Chen, T., & Kaviyarasu, K. (2021). Biosynthesis, characterization, and antibacterial activity of gold nanoparticles. *Journal of Infection and Public Health*, *14*(12), 1842–1847.

Bensy, A.D.V., Christobel, G.J., Muthusamy, K., Alfarhan, A., & Anantharaman, P. (2022). Green synthesis of iron nanoparticles from *Ulva lactuca* and bactericidal activity against enteropathogens. *Journal of King Saud University - Science*, *34*(3), 101888.

Viswanathan, S., Palaniyandi, T., Shanmugam, R., Karunakaran, S., Pandi, M., Abdul Wahab, M.R., Baskar, G., Rajendran, B.K., Sivaji, A., & Moovendhan, M. (2024). Synthesis, characterization, cytotoxicity, and antimicrobial

studies of green synthesized silver nanoparticles using red seaweed *Champia parvula*. *Biomass Conversion and Biorefinery*, *14*(6), 7387–7400.

Kannan, R.R.R., Arumugam, R., Ramya, D., Manivannan, K., & Anantharaman, P. (2013). Green synthesis of silver nanoparticles using marine macroalga *Chaetomorpha linum*. *Appl. Nanosci.*, *3*, 229–233.

Acharya, D., Satapathy, S., Somu, P., Parida, U.K., & Mishra, G. (2021). Apoptotic effect and anticancer activity of biosynthesized silver nanoparticles from marine algae *Chaetomorpha linum* extract against human colon cancer cell HCT-116. *Biol. Trace Elem. Res.*, *199*, 1812–1822.

Somu, P., Khanal, H.D., Gomez, L.A., Shim, J.J., & Lee, Y.R. (2022). Multifunctional biogenic Al-doped zinc oxide nanostructures synthesized using bioreductant *Chaetomorpha linum* extricate exhibit excellent photocatalytic and bactericidal ability in industrial effluent treatment. *Biomass Convers. Biorefin.* DOI: 10.1007/s13399-022-03177-7.

Trivedi, S., Alshehri, M.A., Aziz, A., Panneerselvam, C., Al-Aoh, H.A., Maggi, F., Sut, S., & Dall'Acqua, S. (2021). Insecticidal, antibacterial and dye adsorbent properties of *Sargassum muticum* decorated nano-silver particles. *South African Journal of Botany*, *139*, 432–441.

Moorthi, P.V., Balasubramanian, C., & Mohan, S. (2015). An improved insecticidal activity of silver nanoparticle synthesized by using *Sargassum muticum*. *Appl. Biochem. Biotechnol.*, *175*, 135–140.

Harinee, S., Muthukumar, K., James, R.A., Arulmozhi, M., Dahms, H.U., & Ashok, M. (2022). Bio-approach ZnO/Ag nano-flowers: Enhanced photocatalytic and photoexcited anti-microbial activities towards pathogenic bacteria. *Materials Today Sustainability*, *18*, 100133.

El Shehawy, A.S., Elsayed, A., El-Shehaby, O.A., & Ali, E.M. (2023). Algae-mediated synthesis and structural characterization of silver nanoparticles from *Laurencia papillosa* and *Galaxaura rugosa*. *Egyptian Journal of Aquatic Biology & Fisheries*, *27*(2), 645–659.

Alarif, W.M., Shaban, Y.A., Orif, M.I., Ghandourah, M.A., Turki, A.J., Alorfi, H.S., & Tadros, H.R.Z. (2023). Green synthesis of TiO_2 nanoparticles using natural marine extracts for antifouling activity. *Mar. Drugs.*, *21*(2), 62.

Esmaeilnejad, B., Samiei, A., Mirzaei, Y., & Farhang-Pajuh, F. (2018). Assessment of oxidative/nitrosative stress biomarkers and DNA damage in *Haemonchus contortus*, following exposure to zinc oxide nanoparticles. *Acta Parasitol.*, *63*, 563–571.

Norouzi, R., Ataei, A., Hejazy, M., & Shahbazi, P. (2019). Acaricidal activity of zinc oxide nanoparticles against *Hyalomma* spp. in vitro. *Nanomedicine Research Journal*, *4*, 234–238.

Mweke, A., Ulrichs, C., Nana, P., Akutse, K.S., Fiaboe, K.K.M., Maniania, N.K., & Ekesi, S. (2018). Evaluation of the entomopathogenic fungi *Metarhizium anisopliae*, *Beauveria bassiana* and *Isaria* sp. for the management of *Aphis craccivora* (Hemiptera: Aphididdae). *J. Econ. Entomol.*, *111*, 1587–1594.

Akutse, K.S., Subramanian, S., Khamis, F.M., Ekesi, S., & Mohamed, S.A. (2020). Entomopathogenic fungus isolates for adult *Tuta absoluta* (Lepidoptera: Gel-

echiidae) management and their compatibility with *Tuta* pheromone. *J. Appl. Entomol.*, *144*, 777–787.

Agbessenou, A., Akutse, K.S., Yusuf, A.A., Ekesi, S., Subramanian, S., & Khamis, F.M. (2020). Endophytic fungi protect tomato and nightshade plants against *Tuta absoluta* (Lepidoptera: Gelechiidae) through a hidden friendship and cryptic battle. *Sci. Rep.*, *10***,** 22195.

Sharma, A., Sharma, S., & Yadav, P.K. (2023). Entomopathogenic fungi and their relevance in sustainable agriculture: A review. *Cogent Food Agric.*, *9***,** 2180857.

Zeina, G., & Laing, M. (2022). Isolation and evaluation of South African isolates of *Beauveria bassiana* (Hypocreales: Cordycipitaceae) on *Rhipicephalus microplus* (Acari: Ixodidae). *Exp. Appl. Acarol.*, *86***,** 157–171.

Alikhani, M., Safavi, S.A., & Iranipour, S. (2019). Effect of the entomopathogenic fungus, *Metarhizium anisopliae* (Metschnikoff) Sorokin, on demographic fitness of the tomato leaf miner, *Tuta absoluta* (Meyrick) (Lepidoptera: Gelechiidae). *Egypt. J. Biol. Pest Control*, *29*, 1–7.

Algotiml, R., Gab-Alla, A., Seoudi, R., Abulreesh, H.H., El-Readi, M.Z., & Elbanna, K. (2022). Anticancer and antimicrobial activity of biosynthesized Red Sea marine algal silver nanoparticles. *Sci. Rep.*, *12*(1)**,** 1–18.

El Kassas, H.Y., & Attia, A.A. (2014). Bactericidal application and cytotoxic activity of biosynthesized silver nanoparticles with an extract of the red seaweed *Pterocladiella capillacea* on the HepG2 cell line. *Asian Pacific J. Cancer Prev.*, *15*(3), 1299–1306.

Verma, H., Singh, P., & Chavan, R. (2014). Gold nanoparticle: Synthesis and characterization. *Vet. World*, *7*(2), 72–77.

Al-Zahrani, S.A., Bhat, R.S., Al Rashed, S.A., Mahmood, A., Al Fahad, A., Alamro, G., Almusallam, J., Al Subki, R., Orfali, R., & Al Daihan, S. (2021). Green-synthesized silver nanoparticles with aqueous extract of green algae *Chaetomorpha ligustica* and its anticancer potential. *Green Processing and Synthesis*, *10*(1), 711–721.

Hassan, M.M. (2014). Influence of protoplast fusion between two *Trichoderma* spp. on extracellular enzymes production and antagonistic activity. *Biotechnol. Biotechnol. Equip.*, *28***,** 1014–1023.

Hassan, M.M., Farid, M.A., & Gaber, A. (2019). Rapid identification of *Trichoderma koningiopsis* and *Trichoderma longibrachiatum* using sequence characterized amplified region markers. *Egypt. J. Biol. Pest Control*, *29*, 13.

Senthamizhlselvan, P., Sujeetha, J.A., & Jeyalakshmi, C. (2010) Growth, sporulation and biomass production of native entomopathogenic fungal isolates on a suitable medium. *J. Biopest.*, *3***,** 466.

Zhang, S., Gan, Y., Xu, B., & Xue, Y. (2014). The parasitic and lethal effects of *Trichoderma longibrachiatum* against *Heterodera avenae*. *Biol. Control*, *72***,** 1–8.

Wadaan, M.A., Khattak, B., Riaz, A., Hussain, M., Khan, M.J., Fozia, F., Iftikhar, A., Ahmad, I., Khan, M.F., Baabbad, A., & Ziaullah, A. (2023). Biological control of *Hyalomma* ticks in cattle by fungal isolates. *Vet. Sci.*, *10***,** 684.

Van Damme, V.M., Beck, B.K., Berckmoes, E., Moerkens, R., Wittemans, L., De Vis, R., Nuyttens, D., Casteels, H.F., Maes, M., Tirry, L., & De Clercq, P. (2016). Efficacy of entomopathogenic nematodes against larvae of *Tuta absoluta* in the laboratory. *Pest Manag. Sci.*, *72*(9)**,** 1702–1709.

Puntener, W. (1981). *Manual for field trails in plant protection*. Agricultural Division, Ciba-Geigy Limited, Basle, Switzerland.

Finney, M.A. (2004). *FARSITE*: Fire area simulator—model development and evaluation. Department of Agriculture, USDA, US.

El Aimani, A., Mokrini, F., Houari, A., Laasli, S., Sbaghi, M., Mentag, R., Iraqi, D., & Sripada, M. (2021). Potential of indigenous entomopathogenic nematodes for controlling tomato leaf miner, *Tuta absoluta* (Meyrick) (Lepidoptera: Gelechiidae) under laboratory and field conditions in Morocco. *Physiological and Molecular Plant Pathology*, *116***,** 101710.

Murugesan, S., Bhuvaneswari, S., Shanthi, N., Murugakoothan, P., & Sivamurugan, V. (2015). Red alga *Hypnea musciformis* (Wulf) Lamour mediated environmentally benign synthesis and antifungal activity of gold nano particles. *Int. J. Nanosci. Nanotechnol.*, *6*(1), 71–83.

Al-Rubaye, H.I., Al-Rubaye, B.K., Al-Abodi, E.E., & Yousif, E.I. (2020). Green chemistry synthesis of modified silver nanoparticles. *J. Phys. Conf. Ser.*, *1664* (1), 1–26.

Kamenarska, Z., Gasic, M.J., Zlatovic, M., Rasovic, A., Sladic, D., Kljajic, Z., Stefanov, K., Seizova, K., Najdenski, H., Kujumgiev, A., Tsvetkov, I., & Popov, S. (2002). Chemical composition of the brown alga *Padina pavonia* (L.) Gaill. from the Adriatic sea. *Bot. Mar.*, *45*(4), 339–345.

Kamada, T., & Vairappan, C.S. (2012). A new bromoallene-producing chemical type of the red alga *Laurencia nangii masuda*. *Molecules*, *17*(2)**.** 2119–2125.

Hamdy, A.E., & Dawes, C.J. (1988). Proximate constituents and lipid chemistry in two species of *Sargassum* from the West Coast of Florida. *Bot. Mar.*, *31*(1), 79–82.

Azizi, S., Namvar, F., Mahdavi, M., Bin Ahmad, M., & Mohamad, R. (2013). Biosynthesis of silver nanoparticles using brown marine macroalga, *Sargassum muticum* aqueous extract. *Materials*, *6*(12), 5942–5950.

Renuka, R., Renuka Devi, K., Sivakami, M., Thilagavathi, T., Uthrakumar, R., & Kaviyarasu, K. (2020). Biosynthesis of silver nanoparticles using *Phyllanthus emblica* fruit extract for antimicrobial application. *Biocatalysis and Agricultural Biotechnology*, *24*(3), 101567.

Nagasundari, S.M., Muthu, K., Kaviyarasu, K., Al Farraj, D.A., & Alkufeidy, R.M. (2021). Current trends of silver doped zinc oxide nanowires photocatalytic degradation for energy and environmental application. *Surfaces and Interfaces*, *23*, 100931.

Kingslin, A., Kalimuthu, K., & Viswanathan, P. (2022). Nanocatalytic efficacy of silver nanoparticles fabricated using *Chaetomorpha antennina* algal extract, their characterization, and its applications. *Journal of Scientific Research*, *14*(1)**,** 343–362.

Tavakol, S., Hoveizi, E., Kharrazi, S., Tavakol, B., Karimi, S., & Sorkhabadi, S.M.R. (2017). Organelles and chromatin fragmentation of human umbilical

vein endothelial cell influence by the effects of zeta potential and size of silver nanoparticles in different manners. *Artificial Cells, Nanomedicine and Biotechnology*, *45*(4), 817–823.

Fatima, R., Priya, M., Indurthi, L., Radhakrishnan, V., & Sudhakaran, R. (2020). Biosynthesis of silver nanoparticles using red algae *Portieria hornemannii* and its antibacterial activity against fish pathogens. *Microbial Pathogenesis, 138*, 103780.

Rajivgandhi, G.N., Ramachandran, G., Maruthupandy, M., Manoharan, N., Alharbi, N.S., Kadaikunnan, S., Khaled, J.M., Almanaa, T.N., & Wen-Jun, L. (2020). Anti-oxidant, anti-bacterial and anti-biofilm activity of biosynthesized silver nanoparticles using *Gracilaria corticata* against biofilm producing *K. pneumonia*. *Colloids and Surfaces A: Physicochemical and Engineering Aspects*, *600*, 124830.

Kuhls, K., Lieckfeldt, E., & Samuels, G.J. (1997). Revision of *Trichoderma* section *Longibrachiatum* including related teleomorphs based on an analysis of ribosomal DNA internal transcribed spacer sequences. *Mycologia*, *89*, 442–460.

Fahmi, A.I., Eissa, R.A., El-Halfawi, K.A., Hamza, H.A., & Helwa, M.S. (2016). Identification of *Trichoderma* spp. by DNA barcode and screening for cellulolytic activity. *J. Microb. Biochem. Technol.*, *8*, 202–209.

Zheng, C.J., Li, L., Zou, J.P., Han, T., & Qin, L.P. (2012). Identification of a quinazoline alkaloid produced by *Penicillium vinaceum*, an endophytic fungus from *Crocus sativus*. *Pharm. Biol.*, *50*(2), 129–133.

Baazeem, A., Alorabi, M., Darwesh, H., Alotaibi, S.S., Nour El-Deen, A., Iqbal, S., & Naqvi, S.A. (2022). Biological control of root-knot nematode (*Meloidogyne javanica*) by potential antagonism of endophytic fungi isolated from Taify roses. *Journal of King Saud University– Science*, *34*, 102329.

Oliveira, D.F., Carvalho, H.W., Nunes, A.S., Silva, G.H., Campos, V.P., Júnior, H.M., & Cavalheiro, A.J. (2009). The activity of amino acids produced by *Paenibacillus macerans* and from commercial sources against the root-knot nematode *Meloidogyne exigua*. *Eur. J. Plant Pathol.*, *124*, 57–63.

Bhat, M.P., Kumar, R.S., Chakraborty, B., Nagaraja, S.K., Babu, K.G., & Nayaka, S. (2024). Eicosane: An antifungal compound derived from *Streptomyces* sp. KF15 exhibits inhibitory potential against major phytopathogenic fungi of crops. *Environmental Research*, *251*(1), 118666.

Wang, J.J., Tian, Z.Y., Zhou, Y.P., Yang, J.F., Gao, X., Chen, H.S., Ma, W.H., & Zhou, Z.S. (2024). Electroantennographic and behavioral responses of the melon fly, *Zeugodacus cucurbitae* (Coquillett), to volatile compounds of ridge gourd, *Luffa acutangular* L. *J. Chem. Ecol.*, *50*, 1036–1045.

Silva, A., Cassani, L., Grosso, C., Garcia-Oliveira, P., Morais, S.L., Echave, J., Carpena, M., Xiao, J., Barroso, M.F., Simal-Gandara, J., & Prieto, M.A. (2024). Recent advances in biological properties of brown algae-derived compounds for nutraceutical applications. *Crit. Rev. Food Sci. Nutr.*, *64*, 1283–1311.

Zheng, H., Du, H., Ye, E., Xu, X., Wang, X., Jiang, X., Min, Z., Zhuang, L., Li, S., & Guo, L. (2024). Optimized extraction of polyphenols with antioxidant and

anti-biofilm activities and LC-MS/MS-based characterization of phlorotannins from *Sargassum muticum*. *LWT*, *198*, 116069.

Mardani-Talaee, M., Razmjou, J., Ajdari, A., Serrão, J.E., & Vivekanandhan, P. (2025). Green synthesis of zinc oxide nanoparticles from *Sargassum ilicifolium* to enhance tomato resistance against *Tuta absoluta*. *Scientific Reports*, *15*, 13596.

Li, W., Xie, X., Shi, Q., Zeng, H., Ou-Yang, Y., & Chen, Y. (2010). Antibacterial activity and mechanism of silver nanoparticles on *Escherichia coli*. *Appl. Microbiol. Biotechnol.*, *85*, 1115–1122.

Marouf, A.E., & Abd-Allah, G.E. (2021). The toxic effect of nano silver on *Spodoptera littoralis*, *Tuta absoluta* and *Liriomyza sativae*. *Global Scientific Journals*, 9(1). 149–159.

Zayed, M.S. (2021). A novel approach of chitosan and its derivatives bioactivity against the pinworm *Tuta absoluta* Meyrick (Lepidoptera: Gelechiidae). *J. of Plant Protection and Pathology, Mansoura Univ.*, *12*(4), 323–330.

Hany, A.F., Hosam, M.K., Hammam, E.G., & Osama, A.F. (2016). Nanosilica and jasmonic acid as alternative methods for control *Tuta absoluta* (Meyrick) in tomato crop under field conditions. *Archives of Phytopathology and Plant Protection*, *49*(13), 362–370.

Ramya, S., Narayanasamy, M., Eaban Eamy, G.L, Chandrasekar, G., & Palanivelan, R. (2023). Biofabrication of iron oxide nanoparticles from green seaweed *Ulva lactuca* and screening for its insecticidal activity. *Preprint* December 6th: https://doi.org/10.21203/rs.3.rs-3627269/v1.

Mkiga, A.M., Mohamed, S.A., Du Plessis, H., Khamis, F.M., Akutse, K.S., & Ekesi, S. (2020). *Metarhizium anisopliae* and *Beauveria bassiana*: Pathogenicity, horizontal transmission, and their effects on reproductive potential of *Thaumatotibia leucotreta* (Lepidoptera: Tortricidae). *J. Econ. Entomol.*, *113*, 660–668.

Contreras, J., Mendoza, J.E., Martínez-Aguirre, M.R., García-Vidal, L., Izquierdo, J., & Bielza, P. (2014). Efficacy of enthomopathogenic fungus *Metarhizium anisopliae* against *Tuta absoluta* (Lepidoptera: Gelechiidae). *J. Econ. Entomol.*, *107*, 121–124.

Abdel-Raheem, M.A., Ismail, I.A., Abdel-Rahman, R.S., Abdel-Rhman, I.E., & Reyad, N.F. (2015). Efficacy of three entomopathogenic fungi on tomato leaf miner, *Tuta absoluta* in tomato crop in Egypt. *J. Agric. Res.*, *1*, 15–21.

Tadele, S., & Emana, G. (2017). Entomopathogenic effect of *Beauveria bassiana* (Bals.) and *Metarhizium anisopliae* (Metschn.) on *Tuta absoluta* (Meyrick) (Lepidoptera: Gelechiidae) larvae under laboratory and glasshouse conditions in Ethiopia. *J. Plant Pathol. Microbiol.*, *8*, 411–441.

Abebe, N. (2019). Review on integrated management of tomato leafminer, *Tuta absoluta* (Meyrick) (Lepidoptera: Gelechiidae) on tomato under field and glass house conditions. *J. Biol. AgriHealth*, *9*(17). 7–13.

Kucharska, K., Pezowicz, E., Tumialis, D., & Barkowska, M. (2011). Effect of silver nanoparticles on the mortality and pathogenicity of entomopathogenic nematodes. *Ecological Chemistry and Engineering A*, *18*, 1065–1070.

Feng, M., Chen, G.B., & Ying, S.H. (2004). Trials of *Beauveria bassiana*, *Paecilomyces fumosoroseus* and imidacloprid for management of *Trialeurodes vaporariorum* (Homoptera : Aleyrodidae) on greenhouse grown lettuce. *Biocontr. Sci. Tech., 14*, 531–544.

Kirthi, A.V., Abdul Rahuman, A., Rajakumar, G., Marimuthu, S., Santhoshkumar, T., Jayaseelan, C., & Velayutham, K. (2011). Acaricidal, pediculocidal and larvicidal activity of synthesized ZnO nanoparticles using wet chemical route against blood feeding parasites. *Parasitol. Res., 109*, 461–472.

Hersanti, L.D., Yusup, H., Levaldo, S.P., & Made, J.I. (2020). The effectiveness of suspension of *Beauveria bassiana* mixed with silica nanoparticles (NPs.) and carbon fiber in controlling *Spodoptera litura*. *AIP Conf. Proc., 2219*, 1-1–080011-6.

Hussain, A. (2021). Compatibility of *Beauveria bassiana* and a plant secondary metabolite: A novel modeling approach to invade host defense for effective control of *Oligonychus afrasiaticus* (McGregor) on date palms. *J. Fungi, 7*, 334.

Lakhdari, W., Benyahia, I., Bouhenna, M.M., Bendif, H., Khelafi, H., Bachir, H., Ladjal, A., Hammi, H., Mouhoubi, D., Khelil, H., Alomar, T.S., AlMasoud, N., Boufafa, N., Boufahja, F., & Dehliz, A. (2023). Exploration and evaluation of secondary metabolites from *Trichoderma harzianum*: GC-MS analysis, phytochemical profiling, antifungal and antioxidant activity assessment. *Molecules, 28*, 5025.